energies

MDPI

Article

Design of a Repetitive Control for a Three-Phase Grid-Tied Converter under Distorted Grid Voltage Conditions

Andrzej Straś *, Bartłomiej Ufnalski and Arkadiusz Kaszewski

Faculty of Electrical Engineering, Institute of Control and Industrial Electronics, Warsaw University of Technology, 00-662 Warsaw, Poland

* Correspondence: andrzej.stras@pw.edu.pl

Abstract: The paper presents a design of repetitive control (RC) in the current control system of a three-phase grid-tied converter. The goal of the control system is to provide sinusoidal input filter currents under the conditions of distorted and asymmetrical grid voltage. A novel design of the RC is presented, in which the repetitive part is not excited by sharp and non-periodic changes of the reference signal, but it enables high-quality performance under periodic disturbance conditions. In the proposed system. RC cooperates with a discrete state feedback controller. An innovative approach to tuning is proposed in which parameters of the repetitive, as well as the state feedback controller, are selected as a result of the optimization process with the use of a particle swarm algorithm. The proposed control system is verified experimentally on a laboratory test bench. The achieved results confirm the high-quality system performance.

Keywords: grid-tied converter; repetitive control; particle swarm optimization; current control

check for updates

Citation: Straś, A.; Ufnalski, B.; Kaszewski, A. Design of a Repetitive Control for a Three-Phase Grid-Tied Converter under Distorted Grid Voltage Conditions. *Energies* **2023**, *16*, 754. https://doi.org/10.3390/en16020754

Academic Editor: Vítor Monteiro

Received: 13 December 2022
Revised: 28 December 2022
Accepted: 30 December 2022
Published: 9 January 2023

Copyright: © 2023 by the authors. Licensee MDPI, Basel, Switzerland. This article is an open access article distributed under the terms and conditions of the Creative Commons Attribution (CC BY) license (https://creativecommons.org/licenses/by/4.0/).

1. Introduction

Grid-tied converters are one of the key elements in modern photovoltaics and wind turbine generating systems [1] or power conditioning units with grid-tied fuel cells [2]. Nowadays, environmental problems combined with technological progress have resulted in interest in clean technologies. Therefore, in recent years, grid-tied converters have been gaining more attention from researchers and the industry. An increasing number of non-linear loads connected to the grid system causes an escalation of the problem of distorted grid voltage. According to [3], the harmonics content in the current injected into the grid should not exceed a certain level. In complex power electronic systems, the grid-tied converter is the element responsible for meeting the requirements of transmission system operators. Therefore, the provision of sinusoidal input currents in the case of distorted grid voltage conditions belongs to the most important issues related to the control of grid-tied converters. For this reason, methods for the limitation and elimination of harmonic content in the power system have attracted the attention of researchers. The harmonics that appear in a grid voltage usually follow a specific frequency pattern, e.g., 6-pulse rectifiers produce $6k \pm (k = 1, 2, \ldots)$ order harmonics. For this reason, internal model principle (IMP)-based periodic control can be used to enhance the quality of the input currents of a grid-tied converter. Multioscillatory control, MOSC (also known as multiresonant control), and repetitive control (RC) belong to this type of control. The use of MOSC in a grid-tied converter application is presented in [4–6]. There are similarities in both techniques, presented in [7,8]. Actually, repetitive control is similar to a parallel connection of a proportional-integral controller and MOSC elements at all harmonic frequencies. Recently, RC has been remarkably improved and used in control systems in such applications as drives with a permanent magnet synchronous motor (PMSM) [9–11], wind turbines [12], photovoltaics [13], uninterruptible power supply (UPS) systems [14], modular multilevel converter (MMC) circulating current suppression [15] or shunt active power filter [16].

Moreover, RC-based methods have been developed to further enhance the performance of a grid-tied converter. Adaptation to variable frequency conditions [17,18], repetitive control for particular harmonics [19] and DFT-based RC, which allows enhancement of transient states by choosing gain at each selected harmonic frequency [20,21], belong to the most important of these. Nevertheless, RC can be further enhanced, for example, by a tuning process. To design a repetitive control system, a linear matrix inequality (LMI) is used in [22,23], a method based on H^{∞} is presented in [24], and a root locus approach is utilized in [25]. The main aim of this paper is the development of an advanced repetitive control system for a grid-tied converter operating under distorted and asymmetrical grid-voltage conditions. The task of the control system is to provide sinusoidal currents in a steady-state and high-quality performance during transient states. To realize this goal, a structure of the overall control system is proposed, and current control system parameters are selected in the process of Particle Swarm Optimization (PSO). This kind of design method has been presented for RC systems for a grid-tied converter in [1,26,27]. Nonetheless, in these publications, the conventional controller that cooperates with the repetitive part (PI or state feedback controller) was designed analytically before the repetitive part of the optimization process took place. Such an approach allows the achievement of a high-performance system; however, it does not guarantee the optimal performance of the overall current control system. Nonetheless, in [26], the RC cooperates with a dead-beat controller, which leads to the system with limited robustness in the presence of input filter parameters uncertainty, which is shown in [1].

In the presented herein approach, fractional delay (FD) filters are used in the structure of the RC [17]. This solution allows precise adjustment to the process frequency. The PSO is utilized to obtain an optimal fractional delay repetitive controller (FDRC) gain, phase lead compensation, a low-pass filter coefficient, as well as dynamics of the current control system with a state feedback controller, which is the main contribution of the paper. The presented method utilizes a piecewise-defined performance index to achieve system stability for plant uncertainty as well as high-quality operation.

The paper presents a repetitive control system for grid-tied converters, such as the one shown in Figure 1. It should be mentioned that the RC part can worsen the system performance when violent changes in a reference signal occur [28]. In the case of a grid-tied converter, only distortion (grid voltage) contains several harmonics. This paper presents a novel approach combining the advantages of a system with RC in the case of a distorted grid voltage and a system without this part in the case of a reference change. The proposed control system is applied to a digital signal controller verified experimentally on a laboratory setup.

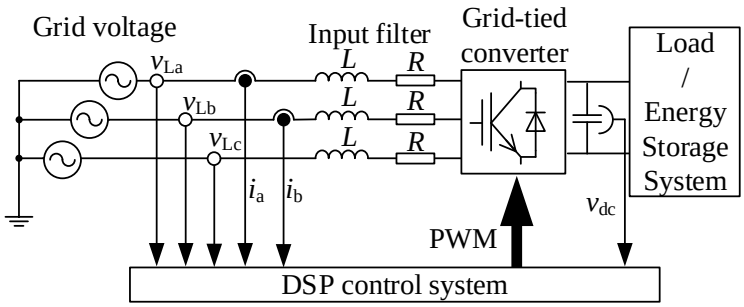


Figure 1. Scheme of the system with a three-phase three-wire grid-tied converter.

This paper is organized as follows. The fundamentals of the system with FDRC, design of discrete current state feedback controller, as well as repetitive control insensitive to reference signal changes, are all presented in Section 2. Section 3 describes the entire control system for a three-phase grid-tied converter, which includes current controller tuning. Section 4 presents the experimental verification of the proposed control, and finally, the conclusion is given in Section 5.

2. Current Control System

2.1. Fractional Delay Repetitive Controller

The block scheme of FDRC is shown in Figure 2, where e is an input of the filter (usually signal error) and u_{RC} is the filter's output. The controller consists of the main path, phase lead path (in positive feedback) and gain. Both paths include delays of integer numbers of samples and fractional delay filters. FD terms approximate the delay of a fractional part of a sample. According to the theory of repetitive control, the overall delay between the controller input and output of the z^{-n_i} element should be equal to the number of samples per repetitive process period. The use of FD1 allows accurate adjustment of the controller to the slowly varying grid frequency. The use of a phase lead track increases the stability range, tracking accuracy and improves the transient response of the system [29]. The implementation of FD2 additionally enhances the precision of the phase lead compensation. In the presented case, the filter is performed in the Farrow structure [30] and is shown in Figure 3, where p_x is the value of the fractional part of the delay. The sub-filters are designed with the use of Lagrange interpolation. The second-order FD filter is used since it provides a higher accuracy than the first-order filter and the higher-order filters can overestimate the amplitude of the signal [1]. Both FD filters have the same structure, and the transfer functions of the sub-filters are $F_0(z) = 1, F_1(z) = -\frac{3}{2} + 2z^{-1} - \frac{1}{2}z^{-2}, F_2(z) = \frac{1}{2} - z^{-1} + \frac{1}{2}z^{-2}$. In the main path, a zero-phase shift low-pass filter is used to provide the selectivity of the controller. The transfer function of the used filter is $Q(z) = \frac{1-\alpha}{2}z + \alpha + \frac{1-\alpha}{2}z^{-1}$. The bandwidth of the filter can be set by choosing the α coefficient. With a higher value of α, the bandwidth of the filter increases accordingly. The transfer function of the FDRC is:

$$G_{FDRC}(z) = k_{RC}\frac{z^{-n_m}G_{FD1}Q(z)}{1 - G_{FD1}(z)G_{FD2}Q(z)z^{-n_m}z^{-n_i}}. \quad (1)$$

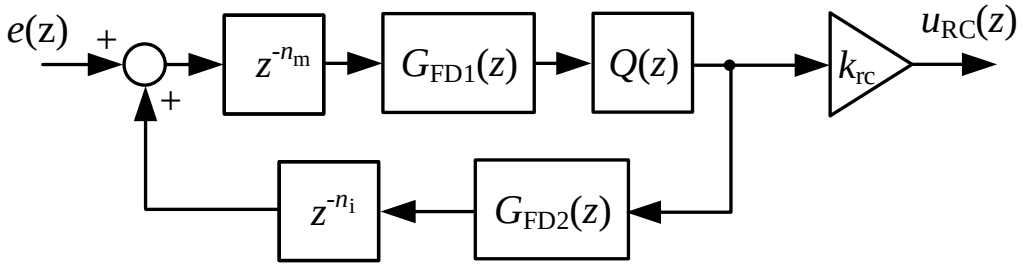


Figure 2. Scheme of the fractional delay repetitive controller.

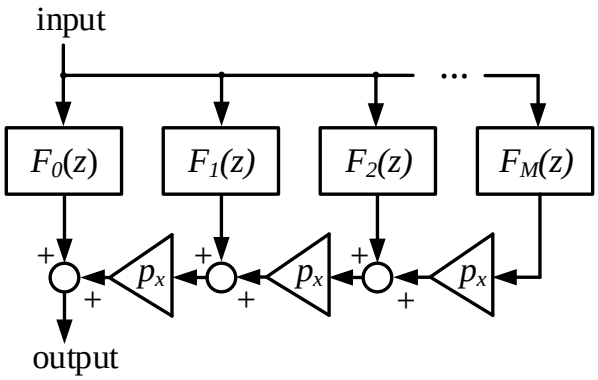


Figure 3. Scheme of a fractional delay approximation using Farrow structure.

The repetitive controller usually cooperates with a conventional controller, for example, PI or state feedback controller. The conventional controller allows a fast response to non-periodic changes in the reference signal, and the repetitive part provides a zero steady-state error for periodic reference/disturbances. In the presented system, FDRC and conventional

controller are implemented in a plug-in structure whose block scheme is shown in Figure 4, where $G_c(z)$ is a transfer function of the conventional controller and $G_p(z)$ is a plant transfer function.

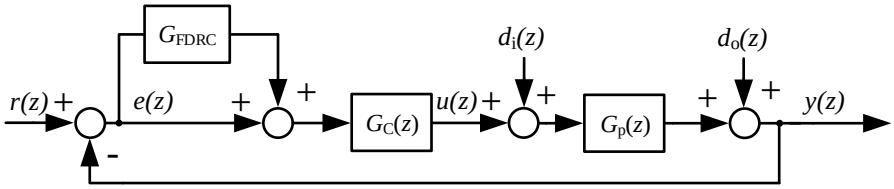


Figure 4. Scheme of the plug-in repetitive control system with FDRC.

2.2. Stability Analysis

The transfer function of the control system without the repetitive controller is:

$$H(z) = \frac{G_c(z)G_p(z)}{1 + G_c(z)G_p(z)}. \tag{2}$$

The transfer function of FDRC can be presented as

$$G_{FDRC} = k_{RC}\frac{A}{1 - AB},$$

where $A = z^{-n_m}G_{FD1}Q(z)$ and $B = z^{-n_i}G_{FD2}$.

Several publications describe the stability analysis for the system that contains a reference signal ($r(z)$) and output disturbance ($d_o(z)$) [17,31–34]. Nevertheless, in the case of a grid-tied converter, the grid voltage is an input disturbance ($d_i(z)$). Since the performance of the control system for the grid voltage changes belongs to the crucial features of the proposed system, the transfer function from $d_i(z)$ to $y(z)$ is also presented herein. According to Figure 4, the transfer functions from $r(z)$ to $y(z)$, $d_i(z)$ to $y(z)$ and $d_o(z)$ to $y(z)$ are:

$$\begin{aligned}\frac{y(z)}{r(z)} &= \frac{(G_c(z)G_p(z))(1 + G_{FDRC})}{(G_c(z)G_p(z))(1 + G_{FDRC}) + 1} = \frac{(G_c(z)G_p(z))(1 + k_{RC}\frac{A}{1-AB})}{(G_c(z)G_p(z))(1 + k_{RC}\frac{A}{1-AB}) + 1} \\ &= \frac{(G_c(z)G_p(z))(1 - AB + Ak_{RC})}{1 + G_c(z)G_p(z) - AB(1 + G_c(z)G_p(z)) + Ak_{RC}G_c(z)G_p(z)} \\ &= \frac{G_c(z)G_p(z)}{1 + G_c(z)G_p(z)} \cdot \frac{1 - AB + Ak_{RC}}{1 - AB + k_{RC}AH(z)}\end{aligned} \tag{3}$$

$$\frac{y(z)}{d_i(z)} = \frac{G_p(z)}{(G_c(z)G_p(z))(1 + G_{FDRC}) + 1} = \frac{G_p(z)}{1 + G_c(z)G_p(z)} \cdot \frac{1 - AB}{1 - AB + k_{RC}AH(z)} \tag{4}$$

$$\frac{y(z)}{d_o(z)} = \frac{1}{(G_c(z)G_p(z))(1 + G_{FDRC}) + 1} = \frac{1}{1 + G_c(z)G_p(z)} \cdot \frac{1 - AB}{1 - AB + k_{RC}AH(z)}. \tag{5}$$

From (3)–(5), the closed-loop FDRC system is stable if the following two conditions are fulfilled:

1. The roots of $1 + G_c(z)G_p(z)$ are inside the unit circle, which means that the control system without FDRC is stable.
2. The roots of $1 - z^{-n_m}G_{FD1}(z)Q(z)z^{-n_i}G_{FD2}(z) + k_{RC}z^{-n_m}G_{FD1}(z)Q(z)H(z)$ are inside the unit circle.

Assuming that $z^{-n_m}G_{FD1}(z) \approx z^{-(n_m+p_m)}$ and $z^{-n_i}G_{FD2}(z) \approx z^{-(n_i+p_c)}$, the expression

$$1 - z^{-n_m}G_{FD1}(z)Q(z)z^{-n_i}G_{FD2}(z) + k_{RC}z^{-n_m}G_{FD1}(z)Q(z)H(z)$$

simplifies to

$$1 - z^{-(n_m + p_m + n_i + p_c)} Q(z)(1 - k_{RC} z^{n_i + p_c} H(z)),$$

where p_m and p_c are delays approximated by FD1 and FD2, respectively. Then, according to the second condition, the system is stable when $||1 - k_{RC} z^{n_i + p_c} H(z)|| < ||\frac{1}{Q(z)}||$ for all $z = e^{j\omega}$, $0 < \omega < \pi$. These stability criteria are compatible with those of a conventional RC system presented in [32].

2.3. State Feedback Controller

In the presented system, the repetitive part cooperates with a state feedback controller. Actually, state feedback control may refer to several approaches to grid-tied converter regulation systems. In [35], it mentions the control system where state variables are DC bus voltage and converter input currents. Another approach is presented in [6], where this term refers to a current feedback control system that utilizes auxiliary terms, for example, integral or resonant elements. In the presented case, state feedback control refers to the current feedback system with a converter delay. Therefore, the accurate design of the controller requires precise identification of the delays that appear in the control system.

The control algorithms of power electronic converters are very often implemented in a digital signal controller in an interrupt service routine, and it is a common practice to sample the measured variables with a fixed period in the reversal points of a triangular modulator waveform. The delay of pulse width modulation (PWM) equals that of a zero-order hold element (ZOH). A microprocessor needs some time to perform computations. Therefore, the control signal that is calculated on the basis of the measurements in the k sample is set out to the PWM registers in $k + 1$. Thus, in the discrete system, the relation between control signal u and voltage generated by the converter v_C (average value for the switching period) is:

$$v_C(k + 1) = u(k). \tag{6}$$

The discrete transfer function of the input filter G_{RL} using ZOH conversion is

$$G_{RL}(z) = (1 - z^{-1}) \cdot Z\{\frac{G_{RL}(s)}{s}\} = \frac{1}{R} \cdot \frac{1 - e^{-\frac{T_s}{\tau_{LR}}}}{z - e^{-\frac{T_s}{\tau_{LR}}}} \tag{7}$$

where R is the filter resistance, τ_{LR} is the filter time constant and T_s is the sampling time. To design the controller, it is convenient to divide an input vector into the vector of control signals **u** and vector of disturbances **d** and an input matrix into control **B** and disturbance **E** matrixes. A discrete state-space model takes the form:

$$\mathbf{x}(k + 1) = \mathbf{A}\mathbf{x}(k) + \mathbf{B}\mathbf{u}(k) + \mathbf{E}\mathbf{d}(k). \tag{8}$$

The coupling between the d and q axes is neglected when designing the controller. Therefore, the state-space model in the discrete domain for one phase is:

$$\begin{bmatrix} i(k+1) \\ v_C(k+1) \end{bmatrix} = \begin{bmatrix} e^{-\frac{T_s}{\tau_{LR}}} & \frac{1}{R}(1 - e^{-\frac{T_s}{\tau_{LR}}}) \\ 0 & 0 \end{bmatrix} \begin{bmatrix} i(k) \\ v_C(k) \end{bmatrix} + \begin{bmatrix} 0 \\ 1 \end{bmatrix} [u(k)] + \begin{bmatrix} -\frac{1}{R}(1 - e^{-\frac{T_s}{\tau_{LR}}}) \\ 0 \end{bmatrix} [v_L(k)]. \tag{9}$$

In the presented case, according to (9), the state vector contains two state variables: current i and voltage generated by the converter v_C and the control vector contains one element u. In the case of current control, a necessity to track a constant reference input is crucial, and therefore, reference gain m is applied. The control law can be expressed as:

$$u(k) = -k_P i(k) - k_T v_C(k) + m i^*(k) \tag{10}$$

where k_P and k_T are gains for the current and voltage, respectively. Since v_C is u delayed by one sample, the realization of the state feedback controller does not require the measurement of the generated voltage. Instead, u value from the previous sample can be used. The block scheme of the state feedback controller (SFC) is shown in Figure 5.

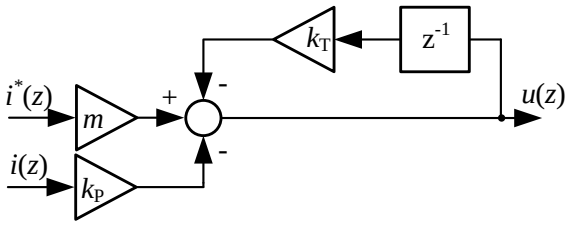


Figure 5. Block scheme of the state feedback current controller.

The general transfer function of the closed-loop system is

$$H(z) = \frac{bm}{z^2 + (k_T - a)z - k_T a + k_P b} \tag{11}$$

where $a = e^{-\frac{T_s}{\tau_{LR}}}$ and $b = \frac{1}{R}(1 - e^{-\frac{T_s}{\tau_{LR}}})$. By selecting controller gains it is possible to locate the pole of the closed-loop system in the demanded place $z_H = e^{-\frac{T_s}{\tau_H}}$ and, therefore, to achieve an aperiodic response from the closed-loop system with time constant τ_H. The transfer function of the closed-loop system is:

$$H(z) = \frac{1 - e^{-\frac{T_s}{\tau_H}}}{z^2 - e^{-\frac{T_s}{\tau_H}} z}, \tag{12}$$

and the controller gains are:

$$m = \frac{R \cdot (1 - e^{-\frac{T_s}{\tau_H}})}{(1 - e^{-\frac{T_s}{\tau_{LR}}})} \tag{13}$$

$$k_T = e^{-\frac{T_s}{\tau_{LR}}} - e^{-\frac{T_s}{\tau_H}} \tag{14}$$

$$k_P = \frac{R \cdot e^{-\frac{T_s}{\tau_{LR}}} (e^{-\frac{T_s}{\tau_{LR}}} - e^{-\frac{T_s}{\tau_H}})}{1 - e^{-\frac{T_s}{\tau_{LR}}}}. \tag{15}$$

The response of the control signal and current for a step of the reference current for $\tau_H = T_s$ is shown in Figure 6.

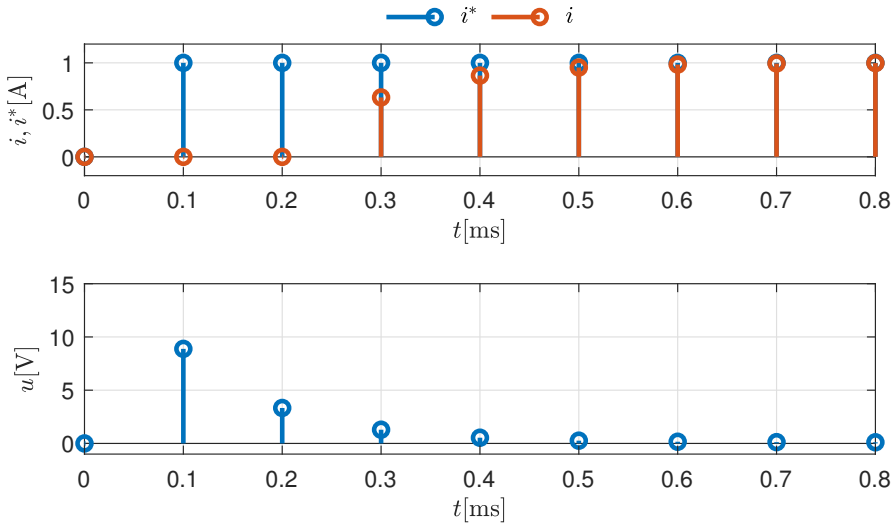


Figure 6. Current response and control signal for a step change in the reference current for a system with $\tau_H = T_s$ (for discrete system, $T_s = 0.1$ ms).

2.4. Repetitive Control Insensitive to Reference Signal Changes

Repetitive control is a suitable solution in the case of a periodic process; however, it may degrade the response of the system in the case of non-repetitive signals. Therefore, in the case of an application where only disturbance contains several harmonics, and the reference is constant, in a steady state it is desired to implement a system that has the following features:

- The response of the system to reference changes is the same as the response without RC. This means that $\frac{y(z)}{r(z)} = H(z)$,
- The response of the system to disturbance changes is the same as the response with RC.

These two features can be obtained by using the system presented in Figure 7. In this structure, the input of the repetitive controller is not directly signal error $e(z)$ but $e_{\mathrm{RC}}(z)$, which is calculated according to:

$$e_{\mathrm{RC}}(z) = r_{\mathrm{RC}}(z) - i(z) \tag{16}$$

$$r_{\mathrm{RC}}(z) = G_{\mathrm{r}}(z) i^*(z) \tag{17}$$

where $G_{\mathrm{r}}(z) = H(z)$. Therefore, the filter G_{r} should have a similar response to reference signal changes in the system without RC.

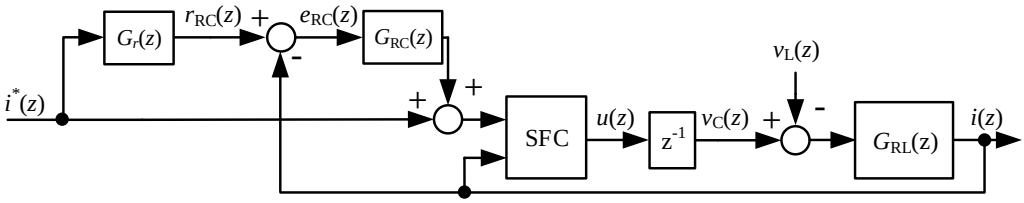


Figure 7. Scheme of the repetitive control insensitive to reference signal changes.

The comparison of the behavior of the conventional repetitive control system and RC insensitive to reference signal changes is shown in Figures 8 and 9. During simulations, the processing period equals $T_{\mathrm{n}} = 10\,\mathrm{ms}$. The response to a unity step of the conventional RC system is shown in Figure 8. The repetitive part allows a constant output in the case of a periodic disturbance. Nonetheless, after a step change in the reference, the RC part causes pulses (visible at $t = 0.06\,\mathrm{s}$ and $t = 0.07\,\mathrm{s}$). Figure 9 shows that using the proposed G_{r} it is possible to avoid the unwanted behavior of the system in the case of non-periodic reference changes and to achieve high-quality performance in the case of a periodic disturbance.

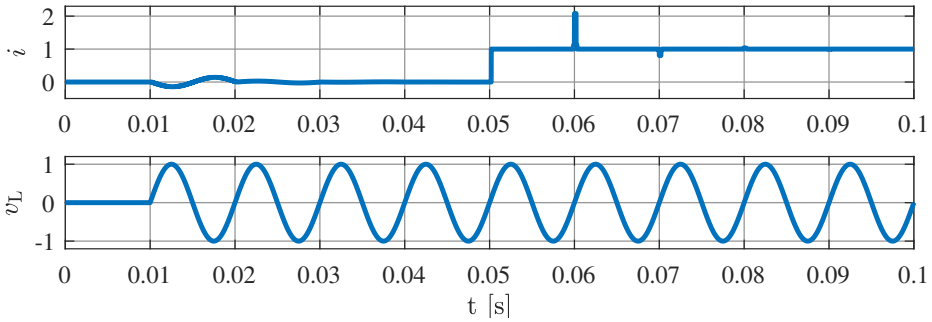


Figure 8. Response of the system to step reference at 0.05 s (output i and periodic disturbance v_{L}) for a conventional plug-in RC system.

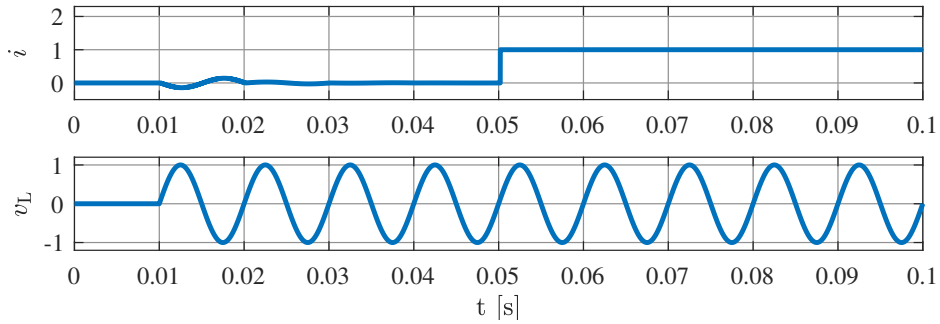


Figure 9. Response of the system to step reference at 0.05 s (output i and periodic disturbance v_L) for a repetitive control insensitive to reference signal changes.

3. Repetitive Control for a Three-Phase Grid-Tied Converter

3.1. Control System Overview

In the presented system, repetitive control is applied in a synchronous reference frame (SRF). The control system is designed with the assumption that the grid voltage is distorted by a 6-pulse rectifier. Thus it contains harmonics of $6k \pm 1$ order and the asymmetry of the fundamental harmonic grid voltage occurs. The aim of the control system is to provide sinusoidal phase currents. Since the FDRCs are applied in the SRF, reference currents are constant in a steady-state, and only disturbance contains several harmonics. Therefore, the G_r filter is used. The scheme of the proposed three-phase grid-tied converter control system is shown in Figure 10. The grid voltage distortion and asymmetry cause a ripple of the DC-link voltage. To achieve symmetrical and sinusoidal input currents, i_d^* must be constant in the steady state. Therefore, the DC-link voltage is filtered by two band-stop filters (BSFs) and one low-pass filter (LPF). The BSFs are used to remove DC-link voltage fluctuations caused by the asymmetry and the fifth and seventh grid voltage harmonics. The rejected frequencies of the BSFs are 100 and 300 Hz. The LPF has a cut-off frequency equaling 500 Hz and is used to attenuate harmonics with higher orders. The voltage PI controller is designed according to the root locus method (a detailed description is shown in [1]).

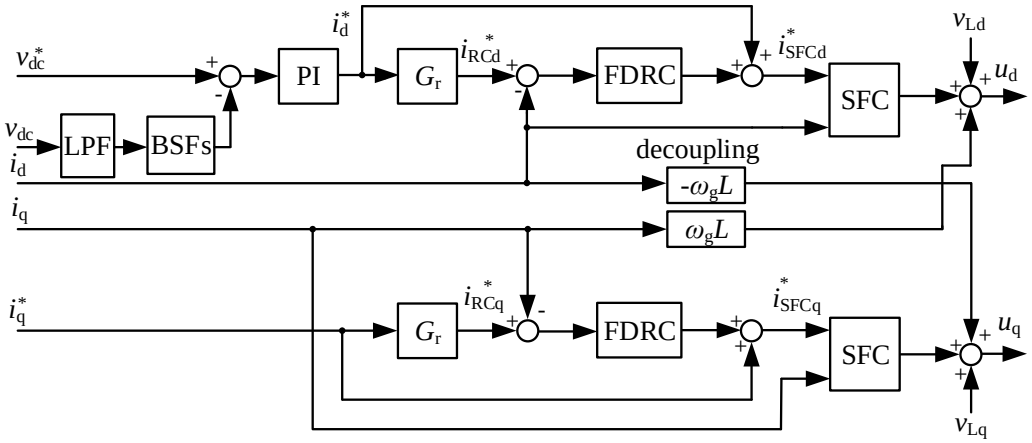


Figure 10. Scheme of the grid-tied converter feedback control system with FDRCs and SFCs.

3.2. Current Control Design

The parameters of the plant are identical in the d and q axes (assuming ideal decoupling). Therefore, the controllers' parameters in both axes are the same. The distortion caused by 6-pulse rectifiers is represented in the dq system by $6k$ order harmonics. However, an asymmetry in the grid voltage is represented by the 2nd harmonic. Therefore, to obtain symmetrical and sinusoidal currents, the base frequency of FDRC is set to $f_b = 2f_g$, where f_g is a grid voltage fundamental frequency. FDRCs, as well as state feedback controllers

gains, are tuned using particle swarm optimization. This tuning approach has already been presented for a repetitive controller in [1,26,27]. Nonetheless, in those publications, only parameters of the repetitive part are optimized and the conventional controller is designed analytically since the optimization of the conventional controller may lead to an unimplementable (too high) gain in the proportional track [36]. In [26], the state feedback controller is designed to achieve a dead-beat response. This approach, combined with an optimized FDRC, also leads to a system with limited stability margins [1]. In the presented case, the parameters of the repetitive, as well as state feedback controllers, are optimized. PSO is used to determine k_{RC}, $Q(z)$ filter α coefficient and phase lead value n_{c} (whose integer part is realized by $z^{-n_{\mathrm{i}}}$ element and the fractional part by FD2) as well as the time constant τ_{H}. On the basis of the time constant, the gains of the SFC are calculated according to (13)–(15). The model for optimization is created in Simulink with the PLECS toolbox and consists of a three phase-circuit and the current feedback control system. The grid-tied converter is modeled as three controlled voltage sources and unit delays introduced into the feedback loop system. The particle swarm algorithm is implemented in Matlab script. The goal of the algorithm is to minimize the performance index:

$$J = \frac{1}{N}\sum_{n=1}^{N}\left(e_{\mathrm{d}}^2(n) + e_{\mathrm{q}}^2(n)\right) \tag{18}$$

where $N = \frac{T_{\mathrm{stop}}}{T_{\mathrm{s}}}$ is the number of samples for one simulation. The natural requirement for the optimization process is that it must provide a stable system. Optimization using a performance index described by (18) allows system stability since instability leads to a great increase in the control error. However, in practice, there are uncertainties in the input filter inductance L and resistance R. Since the stability should also be provided in the case of a mismatch of the plant parameters, the requirement for the optimizer is to provide stability for the system with deviated parameters of the input filter. In the presented method, performance index calculation takes place in two stages:

- First, the stability of the system with deviated parameters is checked. If the system is unstable, the performance index equals infinity. The stability is checked using the *isstable* command for a single-phase model implemented in Matlab script.
- Secondly, if the system with deviated parameters is stable, simulation is performed normally and the performance index is calculated according to (18).

The stability is checked for filter inductance equaling $0.5L$ and resistance $0.5R$. Values lower than the one identified are chosen since this is the crucial situation for current control system stability [1]. During optimization, the system response for variable grid voltage conditions is tested. The test cycle time equals 1.0 s. During the test cycle, the asymmetry of the fundamental harmonic is introduced at $t = 0.1$ s, and from $t = 0.7$ s the voltages are symmetrical again. Moreover, a change from sinusoidal to distorted voltage appears at $t = 0.2$ s and at $t = 0.8$ s the voltage returns to a sinusoidal shape. The amplitudes of all harmonics of the grid voltages, as well as converter parameters, are shown in Table 1.

The optimization is performed for 60 particles and 40 iterations. These values allow the achievement of similar results for different initial particle positions. The achieved values, as well as state feedback controller gains calculated according to τ_{H}, are shown in Table 2.

The currents for the achieved optimal parameters during test cycles are shown in Figure 11 and zoomed-in in Figure 12. It can be seen that after a change in the grid voltage shape, the transient states last about 0.04 s. Then, the currents return to the sinusoidal shape. The transient state after the introduction of the asymmetry of the main harmonic lasts a similar time.

Table 1. Harmonics amplitudes and converter parameters used during the optimization process.

Symbol	Value	Description
f_g	50 Hz	grid fundamental harmonic frequency
v_{L1}	325 V	fundamental harmonic amplitude
v_5	$0.06 \cdot v_{L1}$	5th harmonic amplitude
v_7	$0.05 \cdot v_{L1}$	7th harmonic amplitude
v_{11}	$0.035 \cdot v_{L1}$	11th harmonic amplitude
v_{13}	$0.03 \cdot v_{L1}$	13th harmonic amplitude
v_{17}	$0.02 \cdot v_{L1}$	17th harmonic amplitude
v_{19}	$0.015 \cdot v_{L1}$	19th harmonic amplitude
v_{-1}	$0.1 \cdot v_{L1}$	1st negative harmonic amplitude
L	1.4 mH	input filter inductance
R	0.1 Ω	input filter resistance
T_s	100 µs	sampling period

Table 2. Parameters of the current control system achieved in the optimization process.

k_{RC}	α	n_c	τ_H	m	k_P	k_T
0.59	0.59	2.56	104 µs	8.67	8.52	0.61

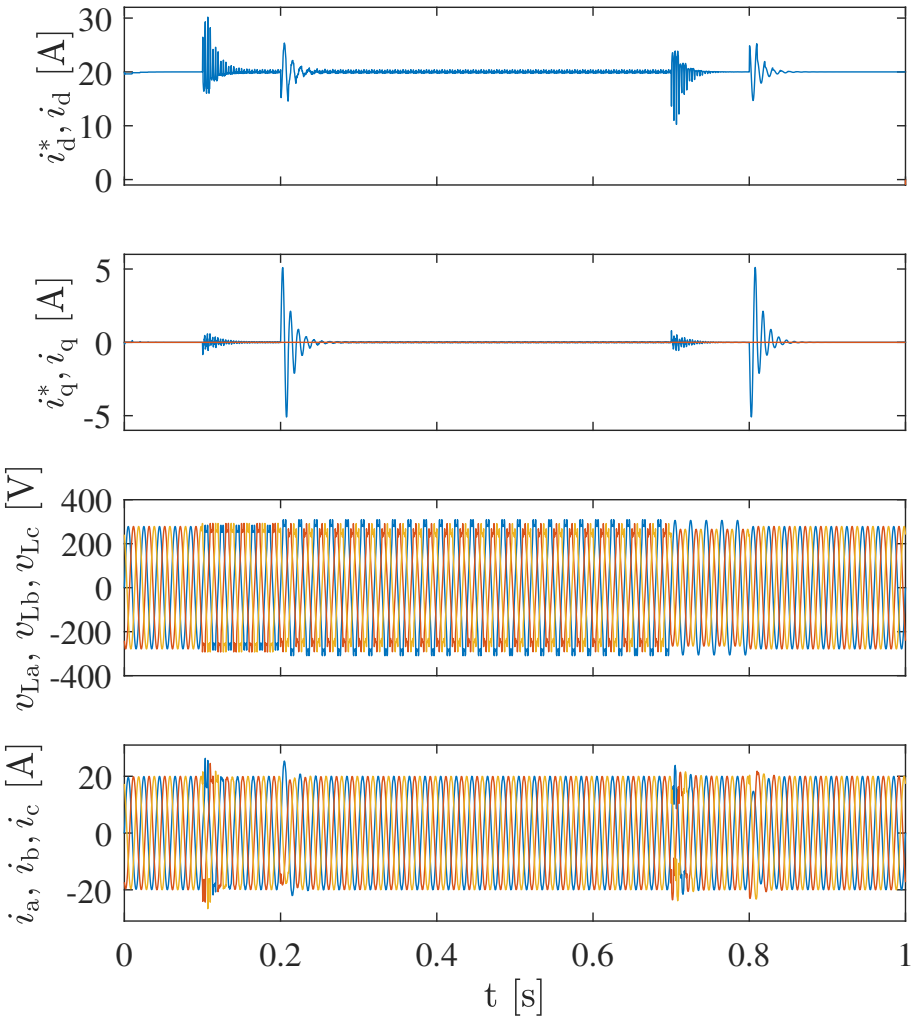


Figure 11. Reference (red) and real (blue) currents in the *dq* system, grid voltages and currents in the *abc* system.

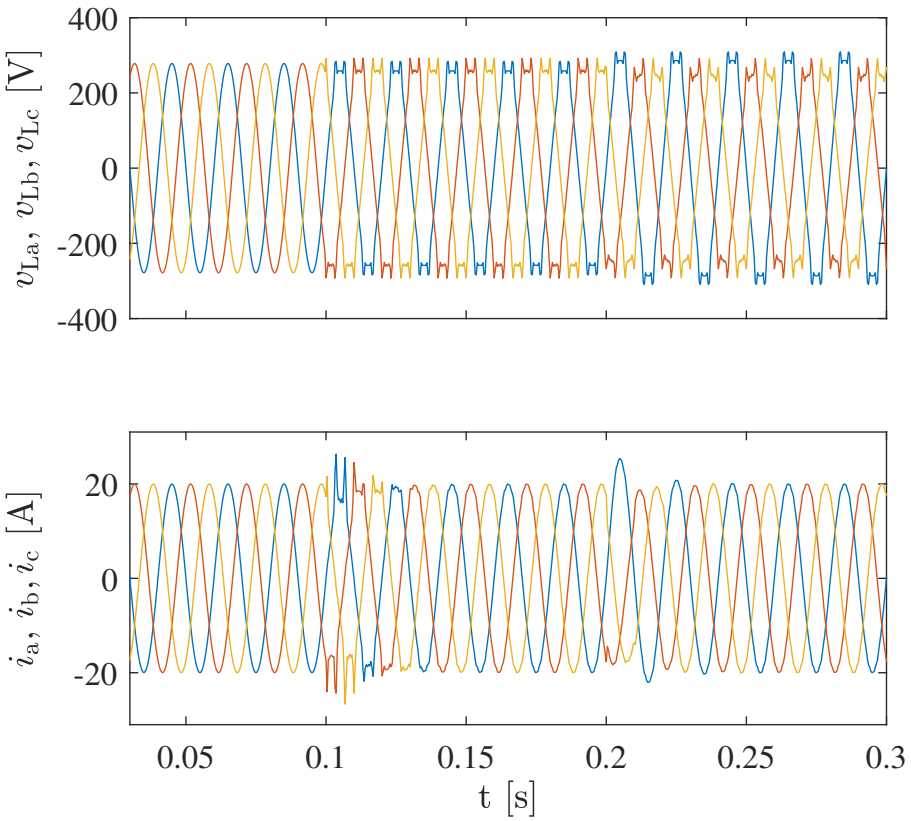


Figure 12. Grid voltages and phase currents (zoom).

4. Experimental Verification

4.1. Laboratory Setup

The laboratory system consists of a three-phase, three-level neutral point clamped (NPC) voltage source converter [37–39] and a two-leg DC/DC converter, which is used to control the load of the DC-link capacitors. The presented control system is implemented on a digital signal controller. The key components and parameters of the setup are listed in Table 3, and the photo of the power electronic converters is shown in Figure 13. To produce distorted voltage, Regenerative Grid Simulator Chroma 61860 is utilized. During the experiments, the parameters of the current controllers are taken directly from Table 2. The phase-locked loop (PLL) described in [7] is used to synchronize the converter control system with the frequency and phase of grid voltages.

Table 3. Parameters and main components of the laboratory system.

Symbol	Value	Description
L	1.4 mH	input filter inductance
R	0.1 Ω	input filter resistance
C	1.5 mF	resulting DC-bus capacitance
T_s	100 µs	sampling and switching period
	IGBT modules	SK150MLI066T
	Gate drivers	CONCEPT 2SC0108T2H0-17
	Current transducers	LEM LA 55-P
	Voltage transducers	LEM LV 25-P
	Digital signal controller	TMS 320F28335

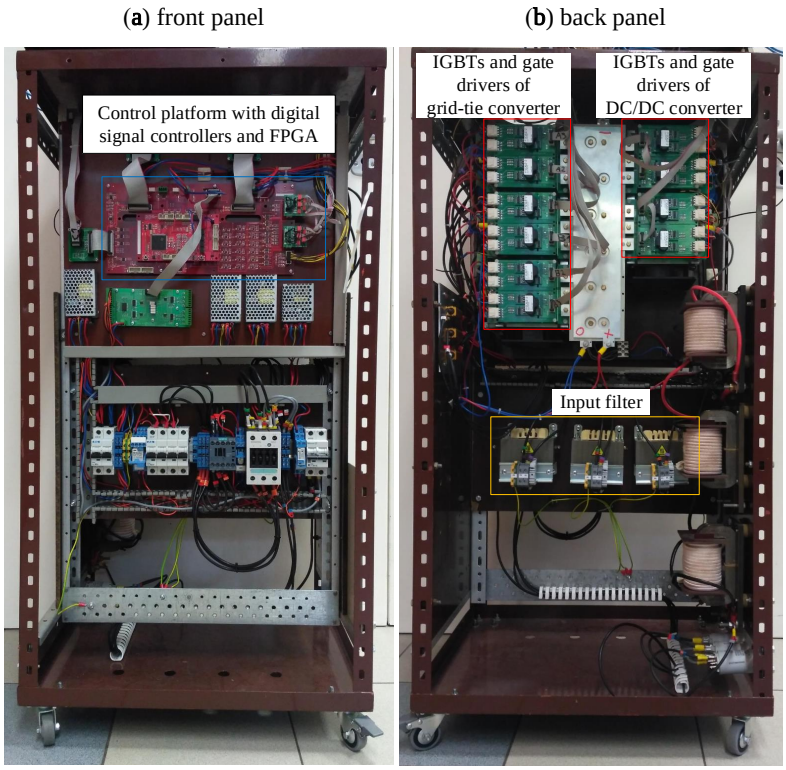


Figure 13. Photo of the power electronic system.

4.2. Steady states

The results for the current control system with a state feedback controller and without RC are shown in Figure 14. It is visible that the currents are far from a sinusoidal shape. The results for the proposed repetitive control system are shown in Figure 15. The results confirm that the proposed RC system provides highly symmetrical and sinusoidal currents. The spectrum of one phase current for the system without and with FDRC is shown in Figure 16. Moreover, the total harmonics distortion (THD) factor up to the 50th harmonic for a current in one phase is calculated. The THD for the system without repetitive parts equals 21.8%, and the THD for the system with FDRC equals 1.5%. The spectrum and THD factors confirm that the content of higher harmonics in the current is remarkably reduced when FDRC is applied.

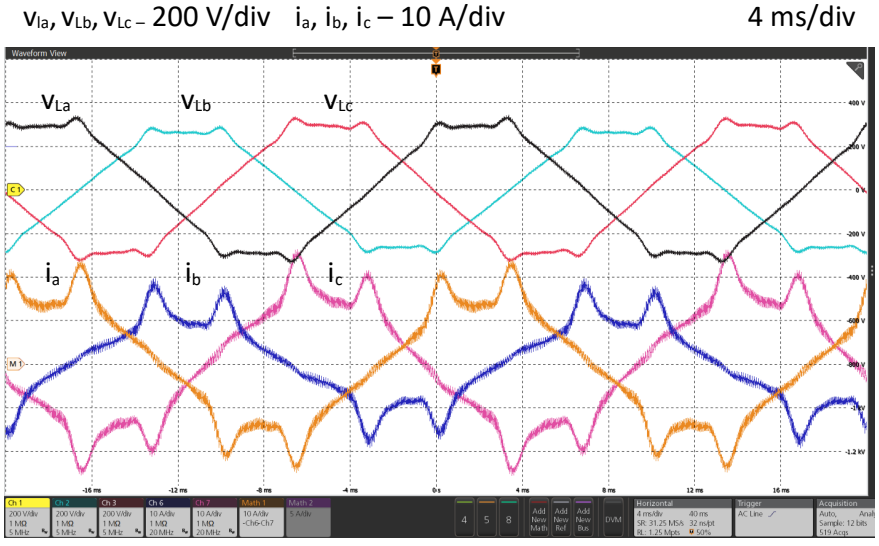


Figure 14. Experimental results of a steady state for the system without repetitive control.

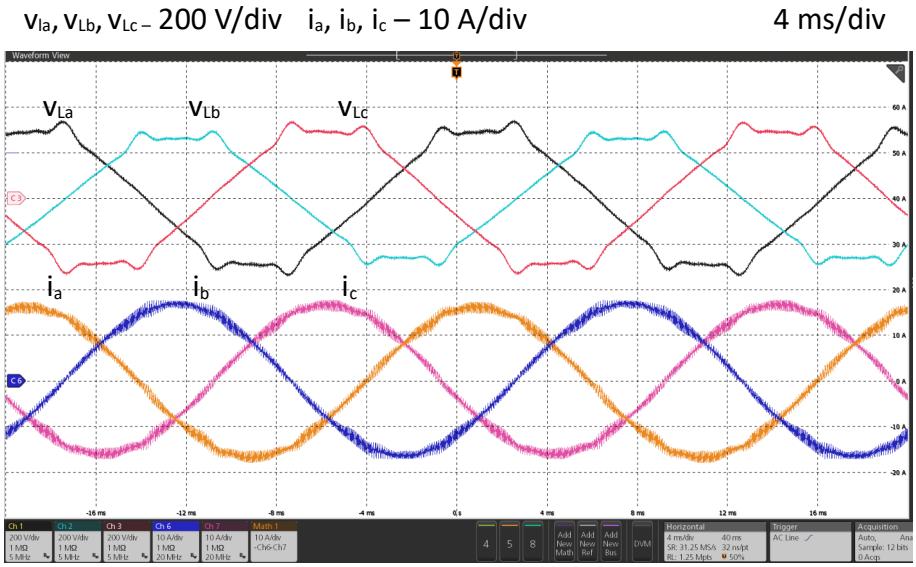


Figure 15. Experimental results of a steady state for the system with FDRC.

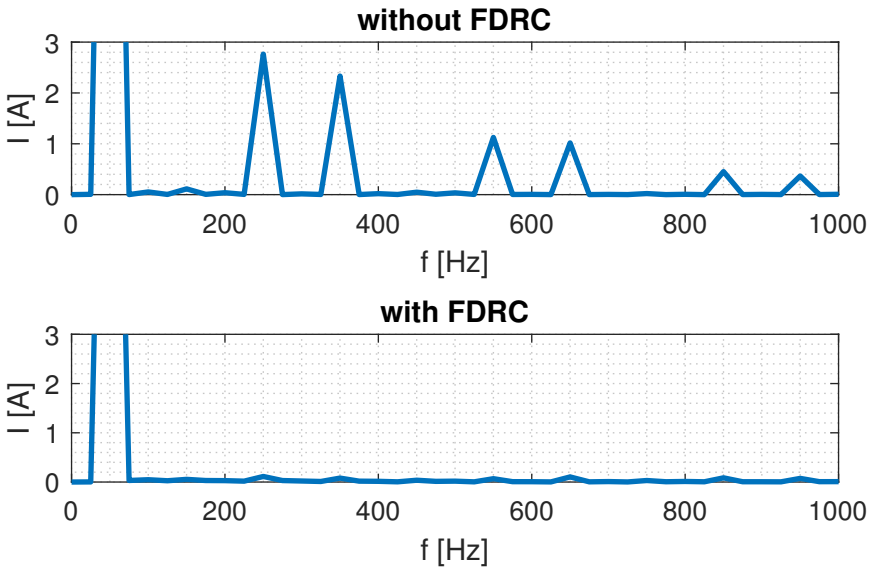


Figure 16. Spectrum of the current of one phase of the grid-tied converter without and with FDRC (experimental results).

4.3. Transient States

Figure 17 presents the response of the system to a fast increase and decrease in the load of the DC-link. The DC-link voltage returns to the reference value after about 30 ms, and during the transient state, the phase currents are sinusoidal.

Figure 18 presents the results of the system in the case of a change in the grid voltage shape from sinusoidal to distorted. The visible transient state lasts about 0.04 s. After this time, the currents are sinusoidal.

The response of the system in the case of an asymmetrical sag is shown in Figure 19. Transient asymmetry is visible for about 0.02 s. Then, after about one period of the grid voltages, the control system provides symmetrical currents.

Figure 20 presents the system performance in the case of a step change in i_q^* for the conventional plug-in RC system. It can be seen that the sinusoidal shape of the currents for the conventional plug-in repetitive control system is distorted (visible 0.01 and 0.02 s after a change in the reference signal). Figure 21 demonstrates the response of the system with G_r

filter: the currents are sinusoidal directly after the change in the reference value. Therefore, this approach should be utilized when RC is only used to deal with a periodic disturbance.

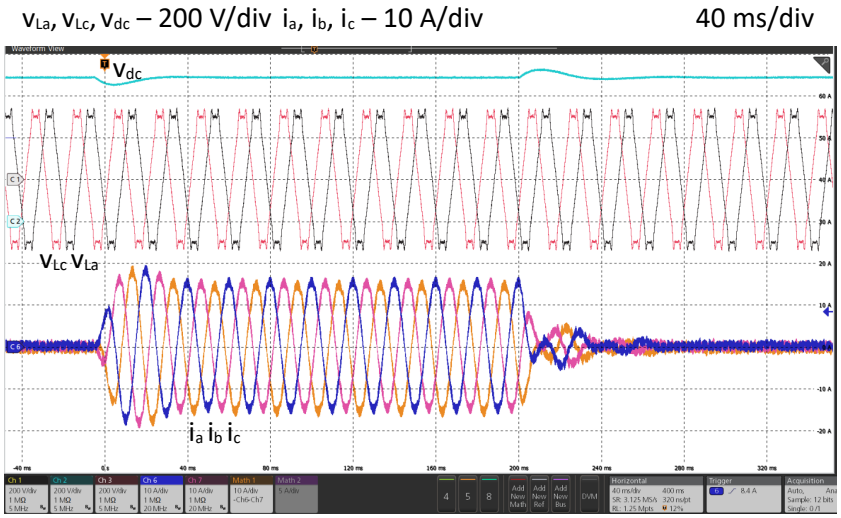


Figure 17. Experimental results of a transient state in the case of DC-link load change.

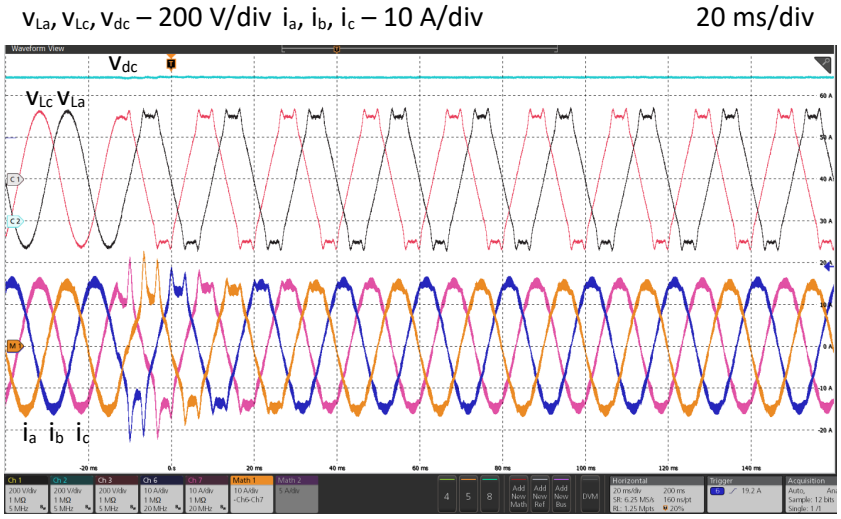


Figure 18. Experimental results for the change in the grid voltage (sinusoidal to distorted).

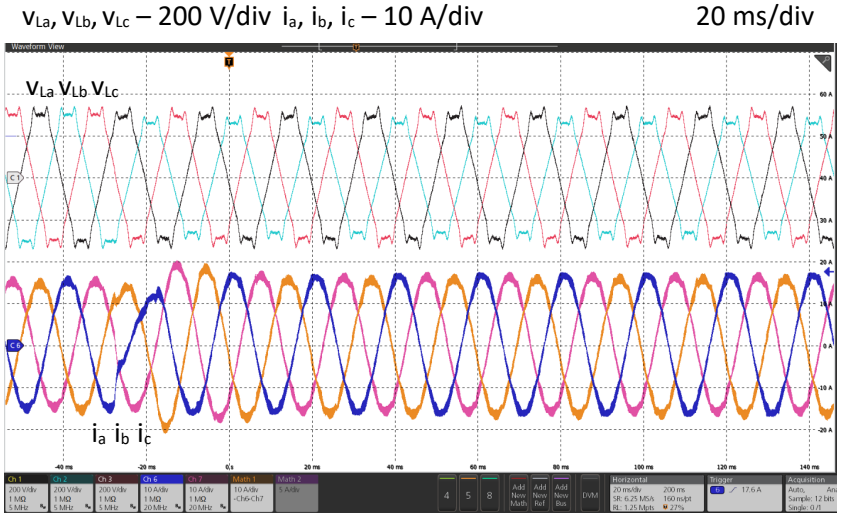


Figure 19. Experimental result of a transient state between symmetrical and asymmetrical grid voltage.

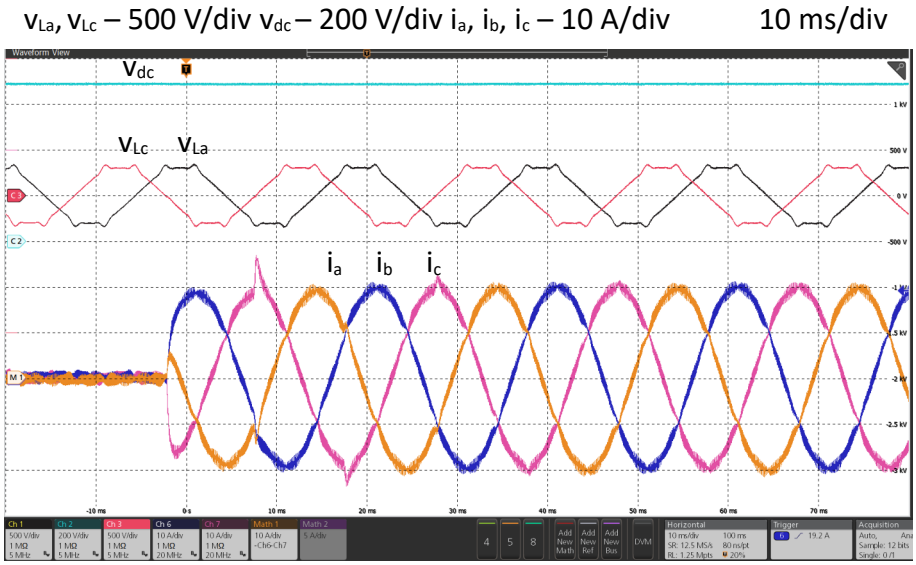


Figure 20. Experimental result for the step change i_q^* for conventional plug-in repetitive control.

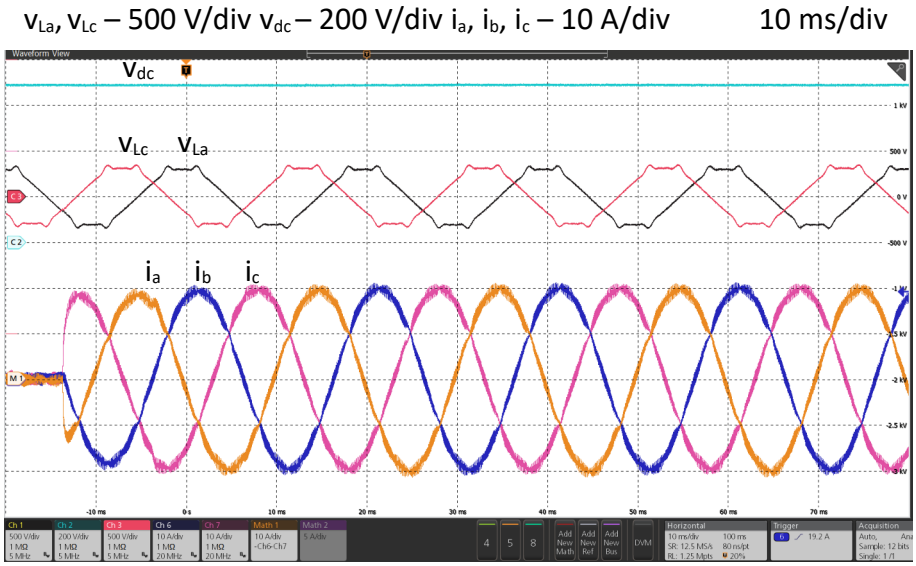


Figure 21. Experimental result for the step change i_q^* for control insensitive to reference signal changes.

5. Conclusions

An original design of a current control system applied in a *dq* system is presented. This approach means that the repetitive control only has to deal with the periodic disturbance and the reference signal is constant in a steady state. This property is used to design a repetitive control insensitive to reference signal changes, which is novel. This approach allows the elimination of an unwanted overshoot in the case of reference signal changes. The parameters of the repetitive, as well as state feedback controller, have been designed using an optimization process that utilizes a particle swarm algorithm. The tuning method provides stability in the case of input filter parameters mismatch. The presented optimization of the dynamics of the closed-loop system with the state feedback controller has proven to be an effective method for state feedback controller design. The viability of the presented method has been demonstrated experimentally.

Author Contributions: Conceptualization, A.S.; methodology, A.S.; software, A.S.; validation, A.S.; formal analysis, A.S. and B.U.; investigation, A.S.; resources, A.S.; data curation, A.S.; writing—original draft preparation, A.S.; writing—review and editing, A.S., B.U. and A.K.; visualization, A.S.;

supervision, B.U. and A.K.; project administration, A.K.; funding acquisition, A.K. All authors have read and agreed to the published version of the manuscript.

Funding: This research was founded by the ENERGYTECH-2 project granted by the Warsaw University of Technology under the program Excellence Initiative: Research University (ID-UB). Agreement number: 1820/41/Z01/POB7/2021.

Institutional Review Board Statement: Not applicable.

Informed Consent Statement: Not applicable.

Data Availability Statement: Not applicable.

Conflicts of Interest: The authors declare no conflict of interest.

References

1. Straś, A. Repetitive Control for a Three-Phase Grid-Tied Converter under Distorted Grid Voltage Conditions. Ph.D. Thesis, Warsaw University of Technology, Warsaw, Poland, 2022.
2. Ben Hamad, K.; Luta, D.N.; Raji, A.K. A Grid-Tied Fuel Cell Multilevel Inverter with Low Harmonic Distortions. *Energies* **2021**, *14*, 688. [CrossRef]
3. *IEEE Std 1547-2003*; IEEE Standard for Interconnecting Distributed Resources with Electric Power Systems. The Institute of Electrical and Electronics Engineers, Inc.: New York, NY, USA, 2003; pp. 1–28.
4. Blaabjerg, F.; Teodorescu, R.; Liserre, M.; Timbus, A.V. Overview of Control and Grid Synchronization for Distributed Power Generation Systems. *IEEE Trans. Ind. Electron.* **2006**, *53*, 1398–1409. [CrossRef]
5. Gałecki, A.; Grzesiak, L.; Ufnalski, B.; Kaszewski, A.; Michalczuk, M. Multi-oscillatory current control with anti-windup for grid-connected VSCs operated under distorted grid voltage conditions. In Proceedings of the 19th European Conference on Power Electronics and Applications (EPE'17 ECCE Europe), Warsaw, Poland, 11–14 September 2017; pp. P.1–P.10.
6. Gałecki, A. Sterowanie 3-fazowym przekształtnikiem AC/DC przy zasilaniu napięciem odkształconym z wykorzystaniem liniowo-kwadratowego regulatora stanu. Ph.D. Thesis, Warsaw University of Technology, Warsaw, Poland, 2019.
7. Jackiewicz, K.; Straś, A.; Ufnalski, B.; Grzesiak, L. Comparative study of two repetitive process control techniques for a grid-tie converter under distorted grid voltage conditions. *Int. J. Electr. Power Energy Syst.* **2019**, *113*, 164–175. [CrossRef]
8. Rashed, M.; Klumpner, C.; Asher, G. Repetitive and Resonant Control for a Single-Phase Grid-Connected Hybrid Cascaded Multilevel Converter. *IEEE Trans. Power Electron.* **2013**, *28*, 2224–2234. [CrossRef]
9. Tang, M.; Gaeta, A.; Formentini, A.; Zanchetta, P. A Fractional Delay Variable Frequency Repetitive Control for Torque Ripple Reduction in PMSMs. *IEEE Trans. Ind. Appl.* **2017**, *53*, 5553–5562. [CrossRef]
10. Tang, Z.; Akin, B. Suppression of Dead-Time Distortion Through Revised Repetitive Controller in PMSM Drives. *IEEE Trans. Energy Convers.* **2017**, *32*, 918–930. [CrossRef]
11. Tang, M.; Formentini, A.; Odhano, S.A.; Zanchetta, P. Torque Ripple Reduction of PMSMs Using a Novel Angle-Based Repetitive Observer. *IEEE Trans. Ind. Electron.* **2020**, *67*, 2689–2699. [CrossRef]
12. Herrán, M.A.; Fischer, J.R.; González, S.A.; Judewicz, M.G.; Carugati, I.; Carrica, D.O. Repetitive Control With Adaptive Sampling Frequency for Wind Power Generation Systems. *IEEE J. Emerg. Sel. Top. Power Electron.* **2014**, *2*, 58–69. [CrossRef]
13. Guo, B.; Su, M.; Yang, J.; Ou, J.; Tang, Z.; Cheng, B.; Liu, M. A hybrid control strategy based on modified repetitive control for single-phase photovoltaic inverter in stand-alone mode. In Proceedings of the IEEE International Conference on Industrial Electronics for Sustainable Energy Systems (IESES), Cagliari, Sardinia, 1–3 September 2018; pp. 308–313.
14. K. Zhang.; Y. Kang.; J. Xiong.; J. Chen. Direct repetitive control of SPWM inverter for UPS purpose. *IEEE Trans. Power Electron.* **2003**, *18*, 784–792. [CrossRef]
15. Yang, S.; Wang, P.; Tang, Y.; Zagrodnik, M.; Hu, X.; Tseng, K.J. Circulating Current Suppression in Modular Multilevel Converters With Even-Harmonic Repetitive Control. *IEEE Trans. Ind. Appl.* **2018**, *54*, 298–309. [CrossRef]
16. Pandove, G.; Singh, M. Robust Repetitive Control Design for a Three-Phase Four Wire Shunt Active Power Filter. *IEEE Trans. Ind. Informatics* **2019**, *15*, 2810–2818. [CrossRef]
17. Nazir, R. Advanced Repetitive Control of Grid Converters for Power Quality Improvement under Variable Frequency Conditions. Ph.D. Thesis, University of Canterbury, Christchurch, New Zealand, 2015.
18. Liu, Z.; Zhang, B.; Zhou, K.; Yang, Y.; Wang, J. Virtual Variable Sampling Repetitive Control of Single-Phase DC/AC PWM Converters. *IEEE J. Emerg. Sel. Top. Power Electron.* **2019**, *7*, 1837–1845. [CrossRef]
19. Lu, W.; Zhou, K.; Wang, D.; Cheng, M. A Generic Digital $nk \pm m$-Order Harmonic Repetitive Control Scheme for PWM Converters. *IEEE Trans. Ind. Electron.* **2014**, *61*, 1516–1527. [CrossRef]
20. Chen, H.; Liu, H.; Xing, Y.; Hu, H. Enhanced DFT-Based Controller for Selective Harmonic Compensation in Active Power Filters. *IEEE Trans. Power Electron.* **2019**, *34*, 8017–8030. [CrossRef]
21. Liu, Z.; Zhang, B.; Zhou, K.; Wang, J. Virtual Variable Sampling Discrete Fourier Transform Based Selective Odd-Order Harmonic Repetitive Control of DC/AC Converters. *IEEE Trans. Power Electron.* **2018**, *33*, 6444–6452. [CrossRef]

22. Ramos, G.A.; Olm, J.M.; Costa-Castello, R. Digital repetitive control under time-varying sampling period: An LMI stability analysis. In Proceedings of the 2009 IEEE Control Applications, (CCA) & Intelligent Control, (ISIC), St. Petersburg, Russia, 8–10 July 2009; pp. 782–787.
23. Ramos, G.A.; Costa-Castelló, R.; Olm, J.M. *Digital Repetitive Control under Varying Frequency Conditions*; Springer: Berlin/Heidelberg, Germany, 2013; Volume 446.
24. Weiss, G.; Hafele, M. Repetitive control of MIMO systems using H^{∞} design. *Automatica* **1999**, *35*, 1185–1199. [CrossRef]
25. Messner, W.; Kempf, C. Zero placement for designing discrete-time repetitive controllers. *Control Eng. Pract.* **1996**, *4*, 563–569. [CrossRef]
26. Straś, A.; Ufnalski, B.; Michalczuk, M.; Gałecki, A.; Grzesiak, L. Design of fractional delay repetitive control with a dead-beat compensator for a grid-tied converter under distorted grid voltage conditions. *Control Eng. Pract.* **2020**, *98*, 104374. [CrossRef]
27. Ufnalski, B.; Straś, A.; Grzesiak, L.M. High quality repetitive control system for a grid-tied converter under distorted grid voltage conditions–design and implementation. *Bull. Pol. Acad. Sci. Tech. Sci.* **2021**, *69*, e136739.
28. Ufnalski, B.; Gałecki, A.; Kaszewski, A.; Grzesiak, L. On the Similarity and Challenges of Multiresonant and Iterative Learning Current Controllers for Grid Converters Under Frequency Fluctuations and Load Transients. In Proceedings of the 20th European Conference on Power Electronics and Applications (EPE'18 ECCE Europe), Riga, Latvia, 17–21 September 2018; pp. P.1–P.10.
29. Yang, Y.; Zhou, K.; Cheng, M.; Zhang, B. Phase compensation multiresonant control of CVCF PWM converters. *IEEE Trans. Power Electron.* **2013**, *28*, 3923–3930. [CrossRef]
30. Eghbali, A.; Johansson, H.; Saramäki, T. A method for the design of Farrow-structure based variable fractional-delay FIR filters. *Signal Process.* **2013**, *93*, 1341–1348. [CrossRef]
31. Zhou, K.; Wang, D.; Yang, Y.; Blaabjerg, F. *Periodic control of Power Electronic Converters*; Institution of Engineering and Technology: 2016. Available online: https://digital-library.theiet.org/content/books/po/pbpo082e (accessed on 12 August 2022)
32. Zhou, K.; Wang, D. Digital repetitive controlled three-phase PWM rectifier. *IEEE Trans. Power Electron.* **2003**, *18*, 309–316. [CrossRef]
33. Zhang, B.; Wang, D.; Zhou, K.; Wang, Y. Linear phase lead compensation repetitive control of a CVCF PWM inverter. *IEEE Trans. Ind. Electron.* **2008**, *55*, 1595–1602. [CrossRef]
34. Liu, T.; Wang, D. Parallel Structure Fractional Repetitive Control for PWM Inverters. *IEEE Trans. Ind. Electron.* **2015**, *62*, 5045–5054. [CrossRef]
35. Guo, Y.; Wang, X.; Lee, H.C.; Ooi, B.T. Pole-placement control of voltage-regulated PWM rectifiers through real-time multiprocessing. *IEEE Trans. Ind. Electron.* **1994**, *41*, 224–230.
36. Straś, A.; Ufnalski, B.; Grzesiak, L. Particle swarm optimization-based gain, delay compensation and filter determination of a repetitive controller for a grid-tie converter. In Proceedings of the 2018 International Symposium on Industrial Electronics (INDEL), Banja Luka, Bosnia and Herzegovina, 1–3 November 2018; pp. 1–7.
37. Nabae, A.; Takahashi, I.; Akagi, H. A New Neutral-Point-Clamped PWM Inverter. *IEEE Trans. Ind. Appl.* **1981**, *IA-17*, 518–523. [CrossRef]
38. Rodriguez, J.; Lai, J.-S.; Peng, F.Z. Multilevel inverters: A survey of topologies, controls, and applications. *IEEE Trans. Ind. Electron.* **2002**, *49*, 724–738. [CrossRef]
39. Straś, A.; Kaszewski, A.; Grzesiak, L. An efficient modulation algorithm for 3-phase NPC voltage source converters. In Proceedings of the 19th European Conference on Power Electronics and Applications (EPE'17 ECCE Europe), Warsaw, Poland, 11–14 September 2017; pp. P.1–P.10. [CrossRef]

Disclaimer/Publisher's Note: The statements, opinions and data contained in all publications are solely those of the individual author(s) and contributor(s) and not of MDPI and/or the editor(s). MDPI and/or the editor(s) disclaim responsibility for any injury to people or property resulting from any ideas, methods, instructions or products referred to in the content.